Solid State Phenomena
ISSN: 1662-9779, Vol. 389, pp 295-303
doi:10.4028/p-vWwaU4

Submitted: 2026-01-23
Revised: 2026-02-24
Accepted: 2026-02-27
Online: 2026-04-16

Local Reinforcement of SPIF-Formed Mg-Zn-Zr Alloy Thin Sheets by TIG Welding

Ecem Ozden[1,a*], Oleksandr Kurtov[2,b], Hans Vanhove[1,c] and Joost Duflou[1,d]

[1]KU Leuven, Department of Mechanical Engineering / Flanders Make, Celestijnenlaan 300B, B-3001 Leuven, Belgium

[2]KU Leuven, Jan Pieter De Nayerlaan 5, B-2860 Sint-Katelijne-Waver, Belgium

[a*]ecem.ozden@kuleuven.be, [b]oleksandr.kurtov@kuleuven.be, [c]hans.vanhove@kuleuven.be, [d]joost.duflou@kuleuven.be

Keywords: Single point incremental forming, Hybrid manufacturing, TIG welding, Magnesium.

Abstract. This study investigates a hybrid manufacturing route combining heat-assisted Single Point Incremental Sheet Forming (SPIF) with Tungsten Inert Gas welding (TIG)-based material deposition for the local reinforcement of Mg–Zn–Zr (ZK61) alloy thin sheets. Flat and curved substrates extracted from SPIF-formed geometries were used to examine the influence of substrate thickness, forming temperature, and geometry on TIG deposition morphology and thermal distortion. The results indicate that heat input and substrate thickness strongly affect deposition morphology and dimensional stability, while SPIF sheet forming temperature influences the repeatability of the deposition process. In addition, deposition behavior exhibited limited sensitivity to substrate curvature for single depositions, whereas successive depositions resulted in increased thermal distortion due to cumulative residual stresses. Overall, this work identifies key process sensitivities and constraints associated with TIG deposition on SPIF-formed magnesium alloy sheets, providing a basis for the development of hybrid forming-deposition process chains for localized reinforcement applications.

Introduction

Single Point Incremental Sheet Forming (SPIF) is a dieless sheet metal forming process in which a clamped sheet is progressively deformed by a numerically controlled tool following a predefined toolpath [1]. Owing to its localized deformation mechanism, SPIF offers high geometric flexibility with low tooling requirements and relatively low forming forces. These characteristics make the process particularly attractive for rapid manufacturing and small-batch production of thin-shell components with complex geometries [1,2].

Despite these advantages, certain applications impose additional functional requirements, such as local thickening and reinforcement, to ensure sufficient structural performance. Such requirements extend beyond the capabilities of incremental sheet forming (ISF) as a stand-alone process, which has motivated growing interest in hybrid manufacturing strategies [3]. In this context, integrating ISF with additive manufacturing (AM) has been proposed as a promising route for local reinforcement and functional tailoring, while maintaining geometric flexibility and limiting additional manufacturing time and cost [3]. Accordingly, integrated hybrid concepts combining SPIF and AM within a single clamping setup have been introduced, including the patented approach reported by Hölker–Jäger et al. [4]. In addition, alternative process sequences, in which SPIF and AM are performed in separate stages, have also been investigated [5,6]. Among these strategies, AM applied after forming is generally considered more compatible with industrial implementation, given the strong dependence of AM-induced material properties on processing strategy and thermal history [3]. Nevertheless, AM on pre-formed sheets introduces challenges related to thermal distortion, interfacial bonding, and toolpath alignment, requiring careful control of the process parameters to maintain dimensional accuracy and structural integrity [3].

For magnesium and its alloys in particular, these challenges are further exacerbated by their low melting point, high susceptibility to oxidation, and rapid solidification rate [7]. These characteristics render magnesium alloys highly sensitive to heat input, increasing the risk of thermal distortion and solidification cracking. This sensitivity, in turn, limits the high-temperature processing window [7,8]. Prior work into the heat-assisted SPIF of Mg–Zn–Zr alloy sheets defined a critical forming temperature range and characterized the effects of forming temperatures and toolpath strategies on the resulting product geometry and material properties [9]. Additionally, a process window for Tungsten Inert Gas (TIG) welding, also known as Gas Tungsten Arc Welding (GTAW), on rolled and annealed Mg–Zn–Zr alloy sheets has been explored, representing an initial step toward post-ISF AM deposition strategies [10]. However, the application of TIG-based material deposition to SPIF-formed components and the influence of SPIF-induced geometrical and thermal history on subsequent deposition behavior remain largely unexplored.

The present study addresses this gap through a preliminary investigation of a hybrid manufacturing route combining heat-assisted SPIF with TIG welding-based material deposition for the local reinforcement of Mg–Zn–Zr alloy thin shells. In particular, the effects of selected SPIF process parameters, namely forming temperature and wall angle, on TIG weld deposition morphology and the resulting thermal distortion of the formed sheets are examined.

Materials and Methods

In this study, ZK61 magnesium alloy sheets in an annealed, hot- and warm-rolled condition were investigated. The chemical composition was Mg–5.3Zn–0.5Zr (wt.%). The sheets had initial dimensions of 225x225 mm and a thickness of 1.6 mm.

Heat-Assisted SPIF setup and forming parameters. Heat-assisted SPIF was conducted using a KUKA KR500MT robotic arm equipped with a non-rotating hemispherical tool (Fig. 1a). Sheet heating was provided by a Nabertherm N210E chamber kiln (11 kW). The sheet-fixture assembly was mounted on a clampable door system using bolted connections, ensuring stable and uniform thermal conditions prior to forming while enabling immediate air cooling upon completion. Details of the temperature monitoring and control strategy are reported in [9].

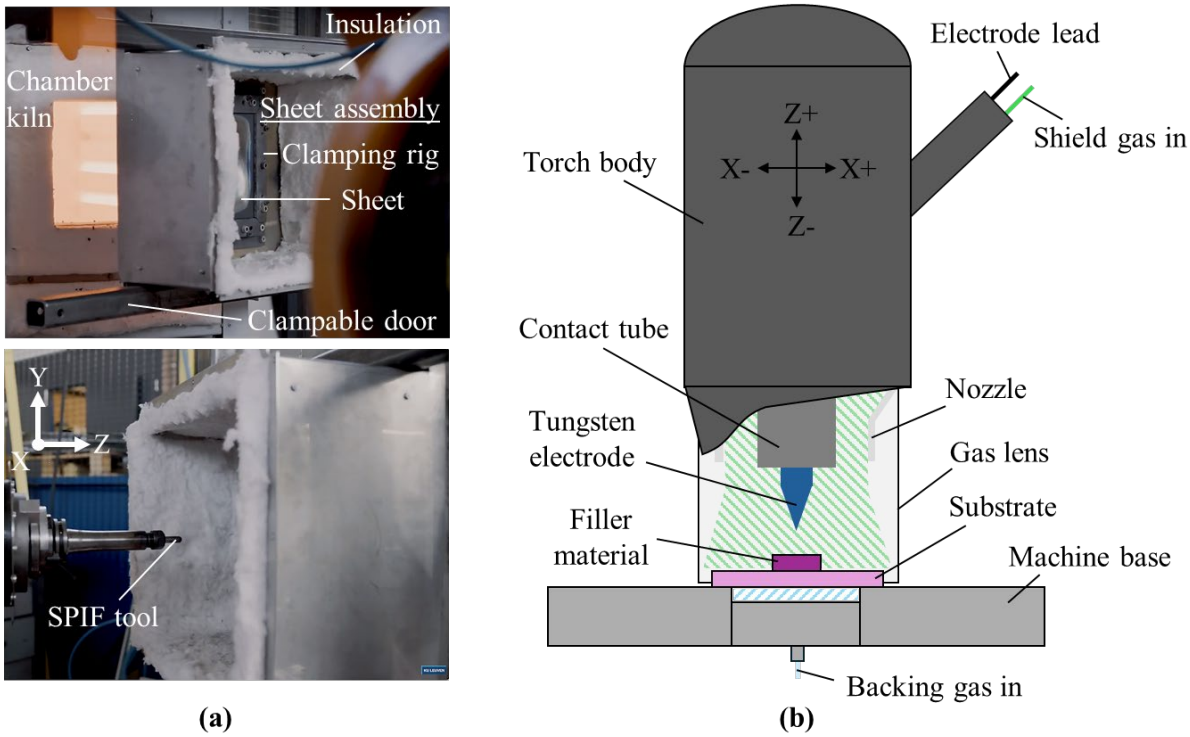

Fig. 1. Experimental setups used in this study: (a) heat-assisted SPIF [9] and (b) TIG welding deposition [10].

Two representative geometries were formed by heat-assisted SPIF using a single-stage toolpath with a constant vertical step size (Fig. 2). Pyramid geometries with varying wall angles were produced at selected forming temperatures to investigate thickness evolution and its influence on subsequent TIG welding when SPIF-formed sheets are used as thin substrates. In addition, cone geometries were produced to enable a direct comparison between flat and curved formed surfaces as substrates for TIG welding.

Two main forming parameters were investigated: sheet temperature and wall angle (Table 1). Based on prior work conducted using the same heat-assisted SPIF setup [9], a forming temperature window of 250–325 °C was selected, as it represents a compromise between enhanced formability, controlled surface oxidation, and acceptable surface quality for Mg–Zn–Zr alloy sheets. Within this temperature range, variations in hardness distribution and grain morphology have been reported, reflecting differences in deformation and recrystallization behavior [9]. Accordingly, forming temperatures were chosen in the present work to introduce controlled differences in the microstructural state of the SPIF-formed substrates. In parallel, the wall angle was varied to produce distinct thickness conditions, which are directly relevant for evaluating thermal distortion during subsequent TIG welding deposition.

All SPIF experiments were performed at a constant feed rate of 2000 mm/min, with a vertical step size of 0.5 mm and a tool diameter of 10 mm, selected to balance surface quality and forming time. No lubricants were applied during forming. Both the pyramid and the cone geometries were formed to a length of 70 mm. The pyramid geometry had an initial width of 184 mm, while the cone geometry had an initial diameter of 180 mm. Prior to forming, the sheets were held at the target temperature for 50 min to ensure steady-state thermal conditions [9]. With the selected parameters, the forming process took approximately 40 minutes, followed by immediate air cooling.

Table 1. Process parameters investigated in the heat-assisted SPIF experiments.

Process parameter	Applied variable
Sheet forming temperature [°C]	250, 325
Wall angle [°]	40, 60

Following forming, flat and curved thin sheets were extracted from the pyramid and cone geometries, respectively, using wire electrical discharge machining (wire EDM). Extractions were performed from a defined region extending from the apex to 55 mm below the apex along the Z direction, corresponding to Zone A in Fig. 2. Regions near the pyramid edges and the step size transition zones were excluded. All extracted sheets had dimensions of 25x20 mm to ensure consistency in subsequent experiments.

Microstructural characterization. Microstructural analysis was performed by optical microscopy on cross-sections of the formed and extracted sheets using a Leica Leitz Laborlux microscope equipped with a Zeiss Axiocam MRC-5 camera. Specimens were prepared using standard grinding and polishing procedures, followed by etching with an acetic-glycol solution to reveal the microstructural features.

TIG welding deposition on SPIF-formed substrates. TIG welding was selected due to its arc stability, flexible heat input control, and inert shielding atmosphere, which effectively suppresses oxidation of molten magnesium [7]. The welding setup (Fig. 1b) consisted of a MacGregor arc power source operating up to 99 A with a current resolution of 0.1 A. Pulsed arc parameters, including peak duration as well as upslope and downslope times, were controlled with a temporal resolution of 1 ms. High-purity argon shielding gas was supplied through a gas lens at the torch, while backing gas was applied at a flow rate of 2 ℓ/min.

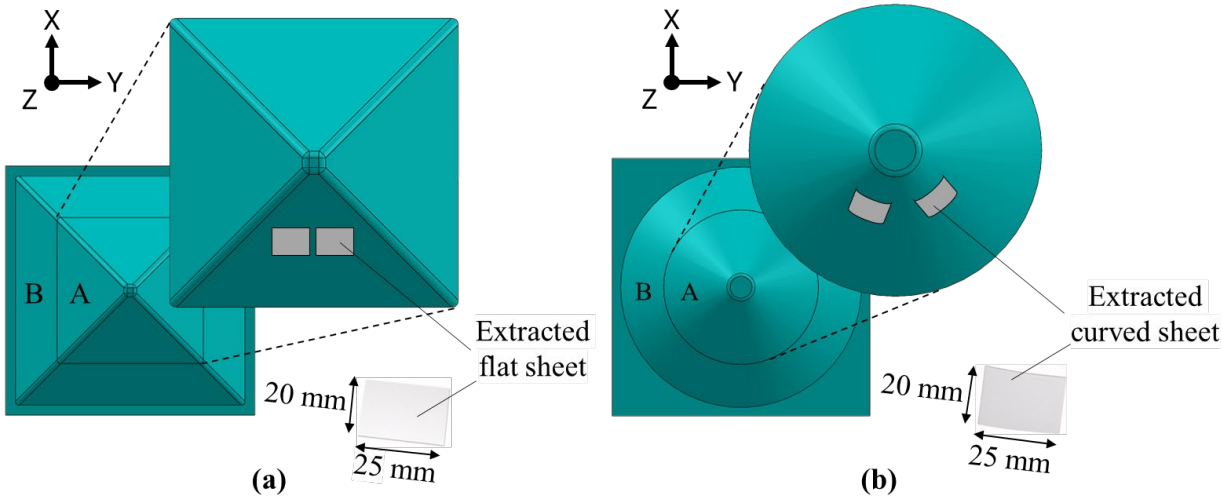

Fig. 2. SPIF-formed geometries used for substrate extraction: (a) pyramid geometry and (b) cone geometry.

Instead of continuous wire feeding, the filler material was positioned centrally on the substrate surface prior to welding. Deposition was carried out at a constant arc length, resulting in dome-shaped weld deposits. The filler material was prepared from the as-received ZK61 sheets with a thickness of 1.6 mm and machined into cylindrical specimens with a diameter of 5 mm using wire EDM.

Prior to welding, both the substrates and filler material samples were sequentially ground using 600, 1200 and 4000 grit abrasive papers and subsequently cleaned with isopropanol to reduce surface oxides and minimize roughness-related effects. Surface preparation removed approximately 0.1 mm of material from each substrate, eliminating surface features such as the orange-peel effect and toolpath marks. As a result, final substrate thicknesses of approximately 1.1 mm and 0.7 mm were obtained for wall angles of 40° and 60°, respectively.

Substrate thickness varied as a function of the SPIF wall angle; therefore, the TIG welding parameters were adjusted accordingly. Substrates formed at a wall angle of 60° were welded using currents of 55 A and welding times of 300–500 ms, whereas substrates formed at 40° required higher currents of 70 A and welding times of 500–800 ms. All other parameters were kept constant: the argon flow rate at the torch was 8 ℓ/min, the upslope and downslope times were 10 ms and 400 ms, respectively, and a tungsten electrode with a 60° tip angle was used at a fixed arc length of 2.4 mm. The electrode condition was inspected after each weld, and at least three repetitions were performed for each parameter set.

The electrode was positioned at a defined distance from the heating contact surface of the sheets, i.e., the surface that was in contact with the heat source during heat-assisted SPIF. The tool contact surface, which was exposed to ambient air and subjected to tool-induced shear during heat-assisted SPIF, was positioned on the back side.

Geometric characterization. To characterize the deposition geometry and thermal distortion, cross-sectional profiles of the substrates were measured before and after TIG welding using a Coord3 MC16 coordinate measuring machine equipped with an LC60Dx laser line scanner. Measurements were performed along the X–Z plane, defined by the TIG welding coordinate system (Fig. 1b), passing through the center of each specimen. Prior to deposition, the extracted and ground thin sheets were scanned to define the initial substrate geometry. Post-deposition scans were conducted after cleaning with isopropanol. Finally, the acquired point clouds were analyzed using GOM Inspect 2019 software.

Results and Discussion

Effect of heat input on cross-sectional deposition geometry. Fig. 3 presents the evolution of the cross-sectional deposition morphology with increasing heat input, controlled by the welding time, on flat substrates extracted from SPIF-formed pyramids with wall angles of 40° (Fig. 3a) and 60° (Fig. 3b). All substrates were produced at a sheet forming temperature of 325 °C. Here, the deposition morphology is characterized in terms of deposition height, deposition diameter, and contact angle. All reported values represent the average of three repeated experiments conducted under identical conditions.

Increasing heat input led to an increase in deposition diameter, accompanied by a reduction in deposition height and contact angle. Specifically, for substrates formed at a wall angle of 40°, increasing the welding time from 500 ms to 800 ms reduced the deposition height from 1.3 mm to 0.4 mm, while the deposition diameter increased from 7 mm to 11 mm. A similar trend was observed for substrates formed at a wall angle of 60°, where increasing the welding time from 350 ms to 450 ms led to a decrease in deposition height from 1.4 mm to 0.7 mm and an increase in deposition diameter from 6 mm to 8 mm.

Additionally, for substrates formed at a wall angle of 60°, no material deposition was obtained at a welding time of 300 ms, indicating insufficient heat input for stable melt pool formation. Conversely, at a welding time of 500 ms, excessive heat input resulted in a pronounced burst formation without the development of a stable dome-shaped deposit. This behavior is consistent with characteristic trends reported for TIG welding, where higher heat input promotes enhanced spreading and penetration of the molten material [11].

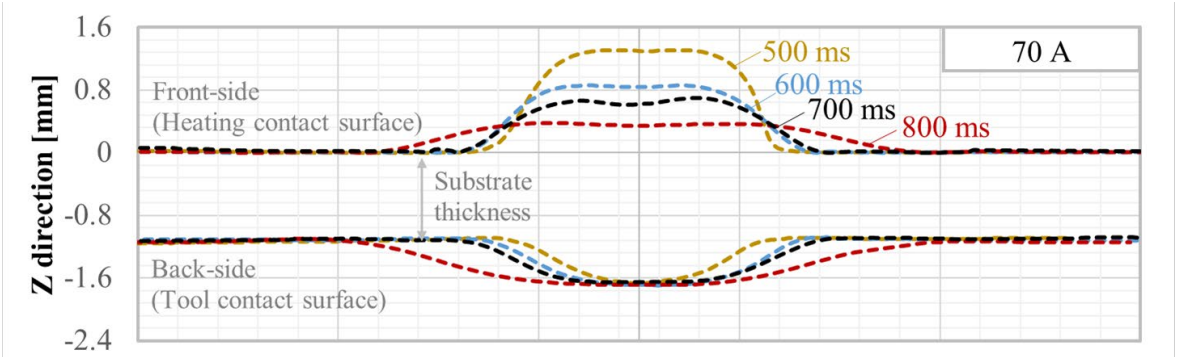

(a) Substrates with a wall angle of 40° formed at 325 °C.

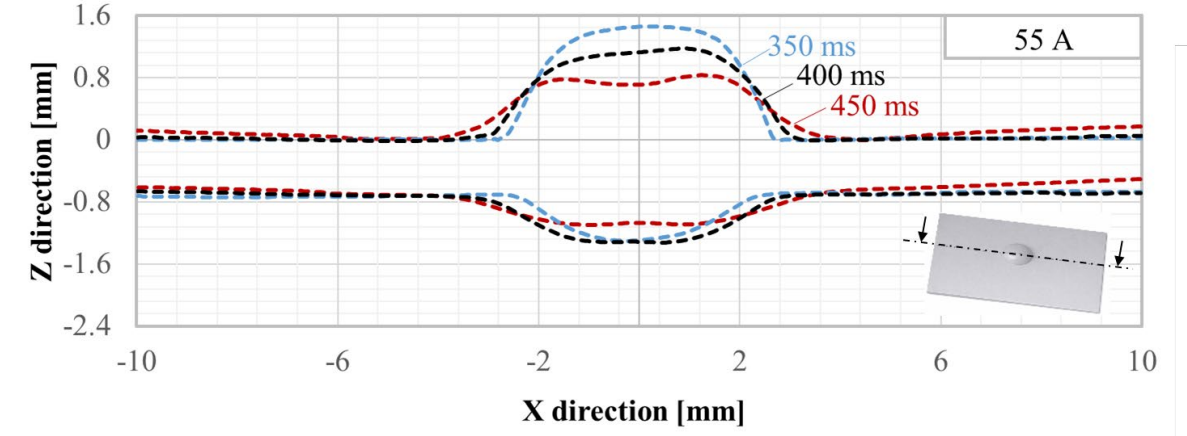

(b) Substrates with a wall angle of 60° formed at 325 °C.

Fig. 3. Cross-sectional deposition profiles at increasing heat input, controlled by the welding time, for flat substrates extracted from SPIF-formed pyramids with varying wall angles.

Influence of substrate thickness and wall angle on thermal distortion. Substrate thickness, governed primarily by the SPIF wall angle, had a pronounced influence on thermal distortion during TIG welding. For substrates formed at a wall angle of 40°, the as-formed thickness after surface

preparation was approximately 1.1 mm. Fig. 3a shows the effect of increasing the welding time from 500 ms to 800 ms at a constant current of 70 A. Within this parameter range, stable dome-shaped deposits were obtained, exhibiting contact angles below 90° and no visible contamination or burst formation. Moreover, the thermal distortion along the X direction remained limited, with the average deviation increasing from ±0.01 mm at a welding time of 500 ms to ±0.02 mm at 800 ms.

In contrast, substrates formed at a wall angle of 60° had a thickness of approximately 0.7 mm, which corresponds to a reduced thermal capacity during TIG welding. As thinner substrates have a reduced ability to absorb and dissipate heat, the heat input must be proportionally reduced to prevent excessive melting, thermal distortion, or burn-through [13]. Accordingly, both the welding current and the welding time were decreased, leading to a markedly narrower process window confined to welding times between 350 ms and 450 ms at a current of 55 A (Fig. 3b).

At welding times of 350 ms and 400 ms, average out-of-plane thermal distortions with deflections of approximately ±0.01 mm and ±0.02 mm, respectively, were observed. When the welding time was increased to 450 ms, the average out-of-plane thermal distortion with a deflection increased to approximately ±0.14 mm was observed over a distance of 12.5 mm from the center of the deposition, relative to the pre-deposition geometry (Fig. 3b). The substrate bent upward toward the deposited region, with the magnitude of deformation increasing with welding time. These observations indicate a loss of dimensional stability, showing that an increase in heat input beyond the narrow process window leads to significant deviation along the Z axis in SPIF-formed thin ZK61 alloy sheets during TIG welding.

Effect of sheet forming temperature on deposition repeatability. Substrates formed at a wall angle of 40° and sheet forming temperatures of 250 °C and 325 °C were subjected to TIG welding deposition using identical process parameters, namely welding times between 500 ms and 800 ms at a constant current of 70 A. For substrates formed at 325 °C, both wall angles of 40° and 60° exhibited reproducible deposition morphology across repeated experiments, with the maximum variations below 0.2 mm in deposition height and 0.3 mm in deposition diameter.

In contrast, substrates formed at 250 °C showed pronounced variability in deposition morphology between repetitions. Variations reached up to 0.7 mm in deposition height and 1.2 mm in deposition diameter, and no consistent weld pool geometry or penetration profile was observed across the experiments. These results indicate a reduced repeatability of the TIG deposition process when applied to substrates formed at the lower forming temperature.

This reduced repeatability in welding morphology for substrates formed at 250 °C can be attributed to the relatively heterogeneous microstructure through the sheet thickness. Forming at 325 °C promotes dynamic recrystallization (DRX), resulting in an equiaxed fine-grain structure with a weakened texture across the thickness (Fig. 4b). In contrast, forming at 250 °C leads to pronounced forming texture characterized by forming stripes with DRX grains (Fig. 4a). This interpretation is consistent with previously reported hardness distributions [9]. Sheets formed at 250 °C had a more pronounced hardness increase near the tool contact surface, where shear deformation dominates during forming. Conversely, samples formed at 325 °C show a more homogeneous hardness distribution through the thickness, consistent with a more homogeneous DRX. Such variations in grain size, crystallographic orientation, and microstructural uniformity have been reported to influence weld pool dynamics, wetting behavior, and solidification characteristics [8], which is consistent with the observed differences in deposition morphology and repeatability in this study.

Nevertheless, the impact of post-forming surface preparation should also be taken into consideration. The grinding steps employed to remove the orange-peel effect and toolpath marks may lead to asymmetric material removal between the heating-contact and tool-contact surfaces, potentially modifying the near-surface microstructural properties. This asymmetry can introduce differences in the near-surface strain state, which may locally affect heat transfer and melting behavior during TIG deposition. A more controlled and symmetric surface preparation strategy on

both sides of the substrate could therefore be considered as an optimization route to further improve the uniformity and repeatability of the deposition morphology within the current TIG welding setup.

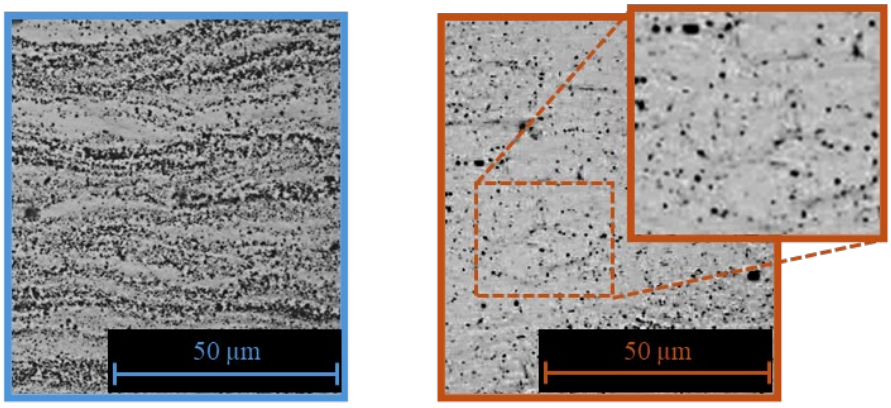

a) Sheet forming temperature of 250 °C **b)** Sheet forming temperature of 325 °C

Fig. 4. Optical micrographs of SPIF-formed pyramid geometries with a wall angle of 40° at different sheet forming temperatures.

Influence of substrate geometry on deposition and distortion. To assess the influence of substrate geometry on deposition behavior and thermal distortion, substrates with curved geometries extracted from SPIF-formed cones were investigated in addition to the thin flat sheets obtained from pyramid geometries. All experiments were conducted within the same TIG welding parameter range to enable a direct comparison between flat and curved substrates. Fig. 5a shows the cross-sectional deposition profiles of cone-derived substrates formed at a wall angle of 40° and a sheet forming temperature of 325 °C.

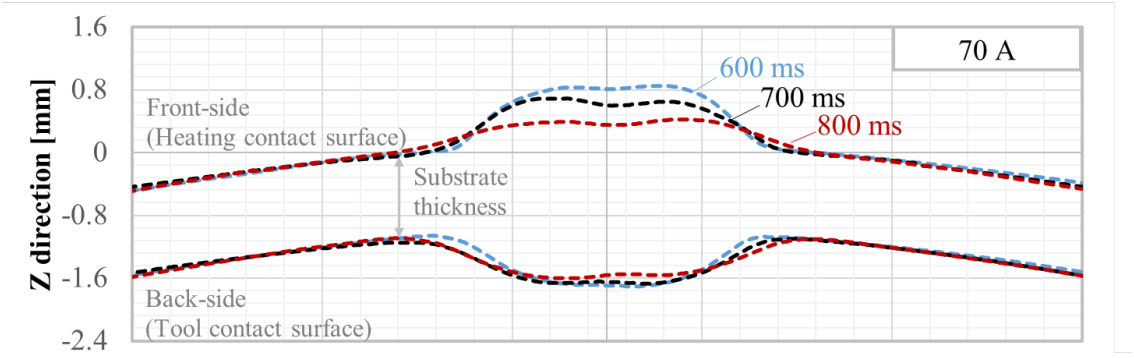

(a) Single deposition under increasing welding time.

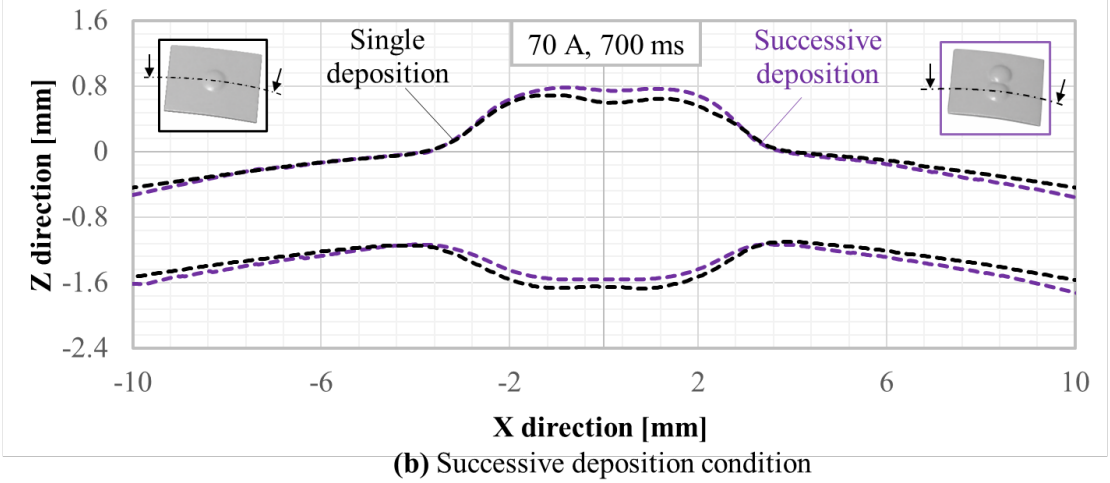

(b) Successive deposition condition applied sequentially on the same curved substrate

Fig. 5. Cross-sectional deposition profiles of SPIF-formed cone-derived substrates with a wall angle of 40° at a sheet forming temperature of 325 °C.

Under identical welding conditions, the cone-derived substrates had deposition morphologies and distortion levels comparable to those observed for the pyramid-derived flat substrates. As the welding time increased from 600 ms to 800 ms, the average deposition height decreased from 0.8 mm to 0.4 mm, while the deposition diameter increased from 8 mm to 11 mm. Moreover, distortion along the X direction remained within a maximum range of approximately ±0.02 mm at 800 ms. These values are consistent with those measured for flat substrates, indicating that the introduction of moderate curvature alone does not significantly alter deposition geometry or thermal distortion under the investigated conditions.

To further evaluate the effect of cumulative residual stresses on the curved substrates, successive depositions were applied on the same cone-derived curve substrate along the Y direction, defined by the TIG welding coordinate system (Fig. 1b). Substrate distortion was evaluated at the same reference position used for the single-deposition case, corresponding to a central dome deposited along the X direction (Fig. 5b). At a welding current of 70 A and a welding time of 700 ms, the successive deposition condition resulted in a noticeably larger out-of-plane displacement exceeding 0.1 mm (Fig. 5b). This result indicates that residual stresses in the workpiece lead to larger deformations when the stress fields from multiple welding spots are combined, resulting in a progressive loss of dimensional stability as the number of deposited domes increases. Consequently, reducing the heat input and/or pre-defining the SPIF geometry to compensate for thermal distortion appear to be potential strategies for continuous or multi-step deposition processes.

Conclusions and Outlook

This study investigated a hybrid manufacturing approach combining heat-assisted SPIF with TIG welding-based material deposition for the local reinforcement of Mg–Zn–Zr (ZK61) alloy thin sheets. The effects of SPIF-induced substrate thickness and forming temperature on TIG deposition morphology and thermal distortion were examined.

The results show that TIG heat input strongly influences deposition geometry, with increasing heat input leading to wider and flatter deposits for all investigated substrate conditions. Substrate thickness, controlled by SPIF wall angle, was identified as a critical parameter governing thermal distortion. Substrates formed at lower wall angles exhibited a comparatively wide and stable TIG welding process window, whereas substrates formed at higher wall angles showed a narrower window beyond which significant out-of-plane distortion occurred.

Forming temperature during SPIF was found to influence the repeatability of TIG welding deposition morphology. Substrates formed at higher temperatures showed consistent deposition morphologies across repeated experiments, while substrates formed at lower temperatures showed pronounced variability, primarily attributed to differences in the microstructural properties of the SPIF-formed sheets across thickness. Within the investigated range, substrate curvature did not significantly affect deposition geometry or distortion for single depositions; however, successive depositions resulted in increased thermal distortion due to the accumulation of residual stresses.

Overall, the findings demonstrate the feasibility of integrating heat-assisted SPIF with TIG-based material deposition for localized reinforcement of magnesium alloy thin sheets. The results highlight the importance of jointly considering deposition morphology and thermally induced distortion when defining a suitable processing window for hybrid SPIF–TIG approaches. While the present study focuses on geometric stability and deposition behavior, further investigation of microstructural and mechanical aspects will be required to fully assess process robustness. Ultimately, the work provides a foundation for future studies addressing continuous deposition strategies and toolpath design for SPIF-formed substrates.

Acknowledgment

This research was conducted within the framework of the STIFF project, facilitated by the KU Leuven C2 research fund.

References

[1] J.R. Duflou, A.M. Habraken, J. Cao, R. Malhotra, M. Bambach, D. Adams, H. Vanhove, A. Mohammadi, J. Jeswiet, Single point incremental forming: state-of-the-art and prospects, Int. J. Mater. Form. 11 (2018) 743–773.

[2] A. Leonhardt, G. Kurz, J. Victoria-Hernández, V. Kräusel, D. Landgrebe, D. Letzig, Experimental study on incremental sheet forming of magnesium alloy AZ31 with hot air heating, Procedia Manuf. 15 (2018) 676–683.

[3] J. Hafenecker, D. Bartels, C.M. Kuball, M. Kreß, R. Rothfelder, M. Schmidt, M. Merklein, Hybrid process chains combining metal additive manufacturing and forming – A review, CIRP J. Manuf. Sci. Technol. 46 (2023) 238–259.

[4] R. Hölker-Jäger, N.A. Ben Khalifa, E. Tekkaya, Method and device for the combined production of components by means of incremental sheet forming and additive methods in one clamping setup, EP Patent 3197633 A1 (2017).

[5] G. Ambrogio, F. Gagliardi, M. Muzzupappa, L. Filice, Additive-incremental forming hybrid manufacturing technique to improve customised part performance, J. Manuf. Process. 37 (2019) 401–411.

[6] C. López, A. Elías-Zúñiga, I. Jiménez, O. Martínez-Romero, H.R. Siller, J.M. Diabb, Experimental determination of residual stresses generated by single point incremental forming of AlSi10Mg sheets produced using SLM additive manufacturing process, Materials 11 (2018) 12.

[7] D.E.P. Klenam, G.S. Ogunwande, T. Omotosho, B. Ozah, N.B. Maledi, S.I. Hango, A.A. Fabuyide, L. Mohlala, J.W. Van der Merwe, M.O. Bodunrin, Welding of magnesium and its alloys: An overview of methods and process parameters and their effects on mechanical behaviour and structural integrity of the welds, Manuf. Rev. 8 (2021) 1–24.

[8] S. Kou, Welding Metallurgy, 3rd ed., Wiley, Hoboken, NJ, 2021.

[9] E. Ozden, H. Vanhove, A. Braem, J.R. Duflou, Heat-assisted single point incremental forming of Mg-Zn-Zr alloy, Mater. Res. Proc. 41 (2024) 1217–1224.

[10] E. Ozden, O. Kurtov, H. Vanhove, J.R. Duflou, Effect of process parameters on local thickening of Mg-Zn-Zr alloy sheets in TIG welding, Mater. Res. Proc. 52 (2025) 281–288.

[11] T. Zhang, C. Xu, J. Cheng, Y. Huang, Y. Peng, L. Wang, K. Wang, Study on droplet transfer behavior and spattering mechanism in Mg–Gd–Y–Zr alloy regulated short circuit (Fronius CMT) welding, J. Manuf. Process. 126 (2024) 35–47.

The publication of this article was funded by the KU Leuven 10.13039/501100004040